Macromolecules
ARTICLE

Macromolecules **2009**, *42*, 6209–6214 **6209**
DOI: 10.1021/ma900971k

Neutron Reflectivity Study of Free-End Distribution in Polymer Brushes

Nikolaos Spiliopoulos,[†] Alexandros G. Koutsioubas,[†,‡] Dimitris L. Anastassopoulos,[†] Alexandros A. Vradis,[†] Chris Toprakcioglu,*[,†] Alain Menelle,[‡] Grigoris Mountrichas,[§] and Stergios Pispas[§]

[†]*Physics Department, University of Patras, Greece 26500,* [‡]*Laboratoire Leon Brillouin, CEA SACLAY, 91191 Gif-sur-Yvette Cedex, France, and* [§]*Theoretical and Physical Chemistry Institute, National Hellenic Research Foundation, 48 Vassileos Constantinou Ave., 11635 Athens, Greece*

Received May 4, 2009; Revised Manuscript Received May 31, 2009

ABSTRACT: In this study, the free-end distribution of a polystyrene self-assembled brush in good solvent (toluene-*d*) is directly probed by use of neutron reflectometry. This is accomplished by the selective deuterium enrichment of polystyrene chains so that all but the last 16% of the monomers of each chain are contrast-matched to the solvent. Thus, only these unlabeled terminal monomers are effectively "visible" to the neutrons. The analysis of the experimental results supports the picture that free ends are not localized at the brush height, but are distributed throughout the brush in agreement with previous theoretical and simulation studies. Detailed comparison is made between the experimentally determined free-end profiles and those predicted by self-consistent field theoretical and simulation models.

Introduction

Polymer chains may become terminally attached to a planar surface either by chemical grafting or physical adsorption of a suitable end-group or anchor-block. In good solvent, when the grafting density is sufficiently high, such tethered chains stretch away from the surface due to excluded volume interactions. The tendency of the chains to stretch is opposed by an elastic restoring force of entropic origin until equilibrium results from a balance between these antagonistic effects, leading to the formation of a "polymer brush".

It is widely recognized that the physical properties of polymer brushes are important for the controllable modification of surfaces and the stabilization of colloidal properties.[1] These practical applications together with fundamental theoretical interest, have spurred numerous theoretical and experimental investigations of various polymer brush systems for over 30 years.[2−12]

The concept of end-grafted polymer chains was first introduced by Alexander in 1977 using a scaling approach.[13] Later in 1980 de Gennes treated such systems using a blob scaling model.[14] In this early scaling theory (often called Alexander−de Gennes theory), the monomer density is assumed to be the same throughout the brush, implying that polymer chains are uniformly stretched and that all chain-ends are located at the edge of the brush.

The Alexander−de Gennes model successfully describes the considerable stretching of overlapping chains and gives the correct scaling law concerning the layer thickness (or "brush height") dependence on molecular weight. However the assumption of the Alexander−de Gennes theory that all chains are equally stretched from the grafting surface is a serious simplification that underestimates the conformational entropy of the grafted polymers.

Several discrepancies originating from this simplification were addressed by the introduction of analytical (aSCF)[15−17] and numerical (nSCF)[18−20] self-consistent-field models by the end of the 1980s, together with numerous Monte Carlo (MC)[21−24] and molecular dynamics (MD)[25,26] simulations. SCF theory (notably the work of Milner, Witten, and Cates[17]) and simulations showed that the monomer volume fraction profile of a brush in a good solvent decreases monotonically away from the surface and has an approximately parabolic form. This prediction has been verified experimentally in many works[11,27−30] for adequately dense brushes by the use of neutron reflectivity experiments. Neutron reflectometry was used because it is a sensitive technique that provides unique information about the volume fraction profile of adsorbed polymers normal to the reflecting surface.[31]

In the SCF model, chain ends are allowed to distribute themselves throughout the brush layer, in contrast to the Alexander−de Gennes picture. Both analytical and numerical results based on SCF theory predict that chain ends populate the whole brush layer even near the grafting surface, while the peak of the chain end distribution is located within the brush layer. In general, MC and MD simulations confirm these predictions with only a minor difference that concerns the existence of a non-vanishing free-end population very close to the surface.

In a recent study the distribution of free ends of an end-grafted polymer layer in the *mushroom* regime has been probed experimentally by the use of grazing incident X-ray standing waves.[32] However, the predictions of simulations and theory have never been experimentally tested for the case of tethered overlapping chains in the *brush* regime. The purpose of the present neutron reflectivity study is to fill this gap by directly measuring the free-end distribution of a self-assembled polystyrene brush in a good solvent such as toluene-*d*. This is accomplished by contrast-matching to the solvent all but the last 16% of the monomers of the polystyrene chains (Figure 1) whose other end is terminally adsorbed onto quartz by means of a zwitterion. We compare the experimentally determined free-end distribution profiles with those predicted by SCF theory, while bond fluctuation Monte Carlo (BFMC) simulations of polymer brushes are also performed in order to gain better insight into the features of our experimental data.

*Corresponding author. E-mail: ctop@physics.upatras.gr.

Published on Web 07/10/2009

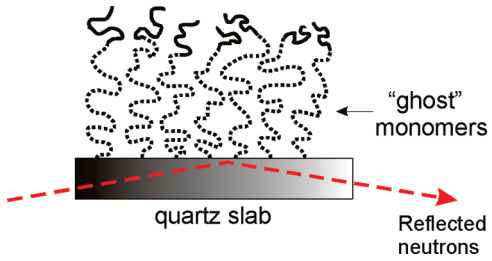

Figure 1. Schematic illustration of the system under study.

Experimental Section

a. Materials. Two PS-X end functionalized polymers, carrying a zwitterionic end-group (X = $(CH_3)_2N^+(CH_2)_3SO_3^-$) were used in this study. The polymers were synthesized by anionic polymerization high vacuum techniques, utilizing (3-dimethylamino)propyllithium as initiator in benzene, and have a narrow molecular weight distribution. The dimethylamino end groups of the polymers were transformed to the polar zwitterionic ones by the postpolymerization reaction with cyclopropanesultone.[33] The first polymer, denoted as "ghost" chain (M_w=77200, M_w/M_n=1.05), was a pseudorandom copolymer, P(S_h-*co*-S_{d8}), consisting of a mixture of deuterated and hydrogenous styrene monomers (13.3% molar hydrogenous styrene, S_h), in order to precisely match the scattering length density of toluene-*d*. The second polymer, denoted as "marked" chain (M_w = 92000, M_w/M_n = 1.04), was a pseudoblock copolymer, which consisted of a block of the previous pseudorandom copolymer, P(S_h-*co*-S_{d8}) (84% molar) and a block of hydrogenous styrene monomer (16% molar). Nondeuterated styrene units were placed at the nonfunctionalized end of the polymer chain, via synthesis. More specifically, a mixture of hydrogenous and deuterated styrene monomer, in the appropriate ratio, was polymerized first and a sample was withdrawn from the reactor ("ghost" chains). Subsequently, a predetermined amount of hydrogenous styrene monomer was introduced in the reactor and allowed to polymerize, giving the "marked" chains.

Molecular weights and polydispersities of the samples were determined by size exclusion chromatography (SEC) using a Waters system, composed of a Waters 1515 isocratic pump, a set of three μ-Styragel mixed bed columns, with a porosity range of 10^2-10^6 Å, a Waters 2414 refractive index detector (at 40 °C), and operated/controlled through Breeze software. Tetrahydrofuran was the mobile phase used, at a flow rate of 1.0 mL/min at 30 °C. The setup was calibrated with polystyrene standards having weight average molecular weights in the range 2500−900000 g/mol. Composition of the polymers were determined by ^{1}H NMR spectroscopy (Bruker MSL 400 spectrometer in $CDCl_3$ at 30 °C), using a polyisoprene homopolymer as an internal standard.

b. Neutron Reflectometry and Data Analysis. Neutron reflectivity measurements were carried out at the Laboratoire Leon Brillouin in Saclay using the EROS time-of-flight spectrometer.[34] The angle of incidence, θ, was 0.75°, and the wavelength was in the range of 2 to 30 Å. The reflectivity was measured as a function of the scattering vector $\vec{Q}$, where $|\vec{Q}| = Q = (4\pi/\lambda)\sin\theta$.

Adsorption was studied on optically flat quartz slabs. Before measurements the quartz substrates were cleaned in 3:1 (v/v) $H_2SO_4-HNO_3$ followed by 3:1 (v/v) $HCl-HNO_3$ for 6 h each. Then, substrates were washed in distilled water followed by a rinse with absolute ethanol. Reflectivity measurements were taken with the aid of a Teflon cell containing the polymer solution and the optically flat quartz slab as substrate.[11] Solutions of the copolymers in toluene-*d* (a good solvent for PS) at a concentration of 0.1 mg/mL were used for adsorption.

From previous studies, it is known that the chains tether to the substrate via the zwitterionic group "X" and that the adsorption process occurs over a period of many hours.[12,35,36]

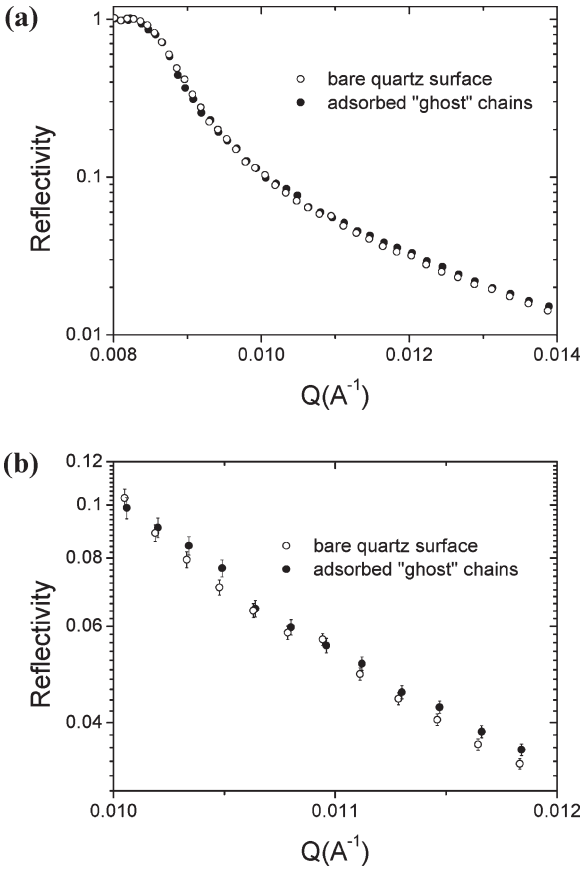

Figure 2. (a) Neutron reflectance of the quartz/toluene interface, before and after "ghost" chain adsorption. (b) Magnification of part a in the scattering vector region 0.010−0.012 Å^{-1}. The error bars of the measured reflectivity are also plotted. Within the experimental error, the presence of "ghost" chains does not cause any measurable change in the neutron reflectivity profile (i.e., the profile after the adsorption of "ghost" chains is essentially identical to the Fresnel reflectivity of the bare quartz/toluene-*d* interface).

It is also known[35] that the adsorbance plateau is reached at very low values of bulk solution concentration and that the final adsorbance attained remains unchanged when the bulk concentration is in the range 5×10^{-2} to 1 mg/mL. In the present experiments, adsorption was allowed to take place for at least 50 h, and measurements were carried out periodically during this time. After the first 12 h of adsorption, subsequent measurements showed no observable change in the volume fraction profiles of the adsorbed polymers. Reflectivity curves were acquired over a period of over 12 h for the sake of statistical accuracy.

Before measuring the reflectivity profiles of the "marked" chains, we checked the effect of "ghost" chain adsorption. As shown in parts a and b of Figure 2, the neutron reflectivity of the quartz surface is not altered, within the experimental error, after the adsorption of ghost chains. This observation implies that the selective deuteration of the PS chains gives a polymer that adequately matches the scattering length density of the toluene-*d* solvent, so that such chains are in effect "invisible" to reflected neutrons.

On the other hand, adsorption of the "marked" chains on the quartz substrate substantially alters the neutron reflectivity of the quartz/toluene-*d* interface, as is illustrated in Figure 3a where the neutron reflectivity profiles for the case of "ghost" and "marked" chain adsorption are plotted. The fact that the last 16% of the marked chains is characterized by very different scattering length density, compared to toluene-*d*, leads to the observed differences in the reflectivity profiles. These differences

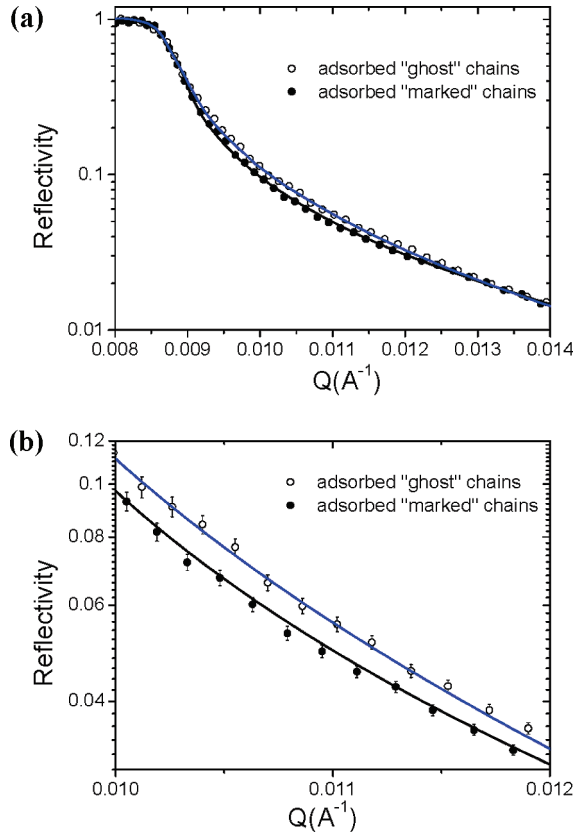

Figure 3. (a) Neutron reflectance of the quartz/toluene-*d* interface, in the case of "ghost" and "marked" chain adsorption. Note the change in the neutron reflectivity profile that is caused by the adsorption of "marked" chains. The two curves represent the results of the fitting procedure: (blue curve) Fresnel fit; (black curve) fit with a modified aSCF model, function B. (b) Magnification of part a in the scattering vector region 0.010−0.012 Å^{-1}. The error bars of the measured reflectivity are also plotted.

are of the order of 15−20% while the statistical error of the measured reflectivity points is of the order of ±1−2%. The range where the differences between the two profiles are most pronounced is approximately between 0.010 and 0.012 Å^{-1}. This is shown in greater detail in Figure 3b.

We stress here that neutron reflectometry is arguably the most suitable method for the investigation of volume fraction profiles given its high resolution and the inherent correspondence between the volume fraction profiles of labeled species and the reflectivity spectrum. Provided that sufficient data are collected so that the statistical error of the measurements is kept low (as is the case in this study and other investigations[28,29,37−40]) neutron reflectometry is a very sensitive probe of the volume fraction profile of adsorbed or grafted macromolecular species.

In order to fit the neutron reflectivity data from adsorbed "marked" chains, we have used various trial end-segment volume fraction profiles that are based on the predictions of SCF theory and MC simulations. As in the case of our previous NR studies,[37−40] the Simplex method was used as a fitting routine to minimize the sum of the weighted squared differences between the experimental points and the fitted reflectivity curves with respect to the fitting parameters. It should be stressed that the data could not be fitted using functional forms that largely deviate from the SCF and MC predicted free-end distribution profile.

c. Simulation Methodology. Bond fluctuation Monte Carlo (BFMC) simulations were performed using the same algorithm that was used by Lai and Binder[21] for the study of polymer brushes in good solvent conditions. We concentrated on monitoring the distribution of the end monomers and of the last 16% of the chains for many different combinations of grafting density σ and chain contour length N.

Briefly, in the BFMC model each monomer occupies a cube of eight lattice sites on a cubic lattice. Each Monte Carlo step involves a random local displacement in one randomly selected direction of a random monomer and the implementation of the excluded volume and bond length criterion. The allowed bond vectors connecting two neighboring monomers may only have a length equal to 2, $\sqrt{5}$, $\sqrt{6}$, 3, or $\sqrt{10}$.[41] The choice of this set of bond vectors ensures that two bonds cannot cross each other.

K linear polymer chains each consisting of N monomers are placed in a $L \times L \times D$ box ($L = 200$, $D = 500$) with one end randomly and irreversibly tethered on the xy plane at $z = 0$. The grafting density is given by $\sigma = 4K/L^2$.[42] All monomers are repelled by the plane at $z = 0$ and periodic boundary conditions are imposed in the directions tangential to this plane.

Chain contour lengths N ranged from 25 to 100 and grafting densities from 0.025 to 0.15. For each set of parameters 10^7 Monte Carlo steps per monomer (MCS) were performed for equilibration followed by 10^7 MCS for the calculation of the end segments profiles.

Results and Discussion

First, an important question that may arise is whether the profile of the last 16% of the grafted chains is representative of the free-end profile of the brush. In fact, aSCF theory [23] predicts the following form for the probability distribution ρ_n of a given monomer n

$$\rho_n(z) = \frac{3z}{\left[h \sin\left(\frac{n\pi}{2N}\right)\right]^2}\sqrt{1-\left[\frac{z}{h \sin\left(\frac{n\pi}{2N}\right)}\right]^2} \times \theta\left[h \sin\left(\frac{n\pi}{2N}\right) - z\right] \quad (1)$$

where z is the distance from the surface, h the height of the brush, N the number of monomers per chain and θ a step function. For the end monomer ($n = N$), eq1 takes the form

$$\rho_{n=N}(z) = \frac{3z}{h^2}\sqrt{1-\left(\frac{z}{h}\right)^2} \times \theta[h-z] \quad (2)$$

In Figure 4, we present numerical calculations based on eqs 1 and 2, for the normalized probability distribution of both the end monomer $\rho_N(z)$ and the last 16% of the chains $\rho_{16\%}(z)$.[43] Note that the two distributions have only minor differences while the position of the peak differs only by 0.7%. Analogous results are also found by the BFMC calculations that were performed. For all combinations of grafting densities and chain lengths studied, $\rho_N(z)$ and $\rho_{16\%}(z)$ have essentially the same form. The peaks of these two distributions have a maximum difference of about 5%, while $\rho_{16\%}(z)$ is slightly less extended in comparison to $\rho_N(z)$. As an example, in figure 5 we present relevant results for a system with $\sigma = 0.1$ and $N = 100$. Based on these results, we may conclude that, by experimentally monitoring the last 16% of the grafted chains, we can in principle get a very good approximation of the free end distribution.

In Figure 6, we present a scaling plot of BFMC determined $\rho_{16\%}(z)$ for different values of the grafting density σ. Although several important features such as the location of the peak approach the SCF predictions, we note that there are some systematic deviations from the theoretical curve that have also been observed in other simulation works.[21] In particular aSCF

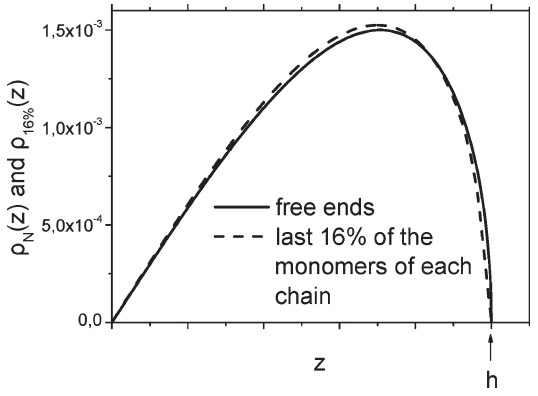

Figure 4. Normalized distribution of free ends and of the last 16% of the monomers of each chain, as predicted by aSCF theory.

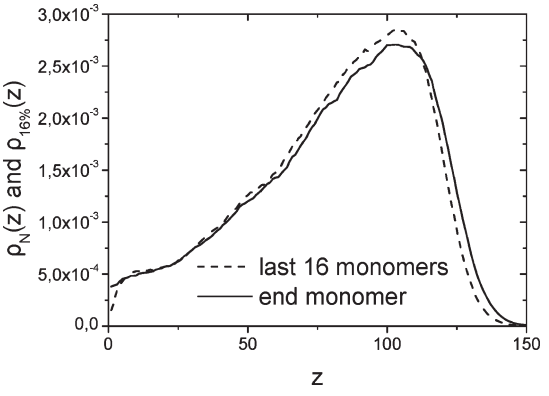

Figure 5. Normalized distribution of the end monomer and of the last 16 monomers as determined by BFMC simulations for system parameters $\sigma = 0.1$ and $N = 100$.

theory predicts that $\rho_{16\%}(z)$ and $\rho_N(z)$ should tend to zero linearly with z, whereas we obtain a nonzero free-end density very close to the surface. Also, the tail of the distribution does not show the abrupt decrease to zero that is predicted by aSCF.

The relatively long tail at the end of the free-end distribution, as in the case of the total volume fraction profile, is a result of the finite number of monomers per chain and has also been predicted by nSCF calculations. However the fact that the end density stays nonzero near the surface is neither found in aSCF nor nSCF results. It is quite possible that this feature would become asymptotically valid for the limit $N \rightarrow \infty$, $\sigma \rightarrow 0$ (keeping $N\sigma^{1/3}$ finite) that is hardly accessible experimentally. Also, note that in figure 6 the concentration of free-ends very close to the surface is dependent on the grafting density of the brush and that the profile is rather convex in the region between $z = 0$ and the position of the peak. A polynomial fit of the profile in this region suggests that a function of the form $a + bz^2$ describes the simulation data very accurately.

We have used both the predictions of SCF theory and BFMC simulations as starting points for the fitting of neutron reflectivity data, concerning the adsorption of the "marked" chains (Figure 3). The first trial function (A) is based on eq 2, which is a pure aSCF profile of the form $\rho_1(z) \sim z(1 - z^2)^{1/2}$. The second trial function (B) is a general modified aSCF profile of the form $\rho_2(z) \sim c + z^n(1 - z^2)$ plus a Gaussian tail at the end of the distribution. Finally the third trial function (C) is a Shultz function of the form $\rho_3(z) \sim c + z^n e^{-azx}$. Parameters n, a, x, and c of functions B and C are left free during the fitting procedure in order to check the BFMC predictions of a nonzero concentration at $z = 0$ and convex nature of the distribution near the surface. We note once again that trial functions that substantially deviate

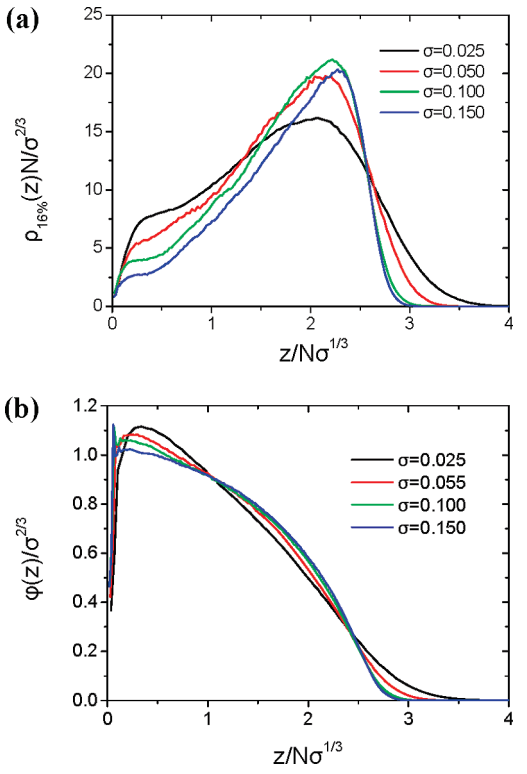

Figure 6. Scaling plot of (a) $\rho_{16\%}(z)$ and (b) the brush volume fraction profile for four different grafting densities, as determined by BFMC simulations. The number of monomers per chain is set equal to 100.

Table 1. Weighted Squared Differences and Total Adsorbed Amount, As Determined by Fits of the Experimental Data Using the Three Different Trial Functions, Described in Text[a]

function (best fit parameters)	weighted squared differences	total adsorbed amount Γ(mg/m^2)
function A	0.936	2.1 ± 0.1
function B ($c = 0.0028$, $n = 2$)	0.802	2.4 ± 0.1
function C ($c = 0.0012$, $n = 2$, $a = 2.6\ 10^{-6}$, $x = 4$)	0.824	2.2 ± 0.1

[a] The best fit parameters for each model are also presented.

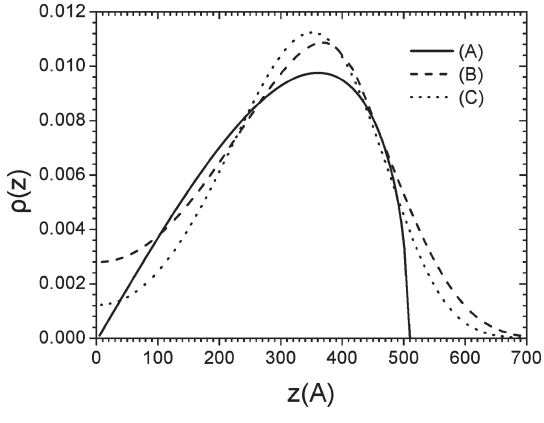

Figure 7. Free end distribution profiles as determined by different fits of the experimental neutron reflectivity curves: (solid curve) SCF theory, function A; (dashed curve) modified aSCF theory, function B; (dotted curve) Shultz function, function C.

from the above-mentioned profiles and do not distribute the free-ends in the whole of the brush layer, give very poor fits, thus

exhibiting very large sums of the weighted squared differences between the experimental points and the fitted reflectivity curves.

In Table 1, we summarize the fitting results (parameters, total adsorbed amount) for each trial function, and in Figure 7, the profiles that give the best fits are plotted. First, we observe that the pure SCF profile (function A) gives a satisfactory fit with a total adsorbed amount equal to 2.1 mg/m^2, close to that found for the other two functional forms. However trial functions B and C give better fits when c is nonzero and when the exponent n takes the value 2. It is quite interesting that this value of the exponent was also found by fits of the BFMC free-end profiles. Also note that the best fit profiles of function B and C tend to have slightly higher adsorbed amounts (2.2 and 2.4 mg/m^2 respectively) and similar forms, while their peaks are closer to the edge of the layer (i.e., the brush height) than to the surface.

It is evident from the fitted experimental results that the free-end distribution of the studied PS brush in toluene tends to deviate from the asymptotic limit predictions of SCF theory primarily in the region near the surface. We get an appreciable free-end concentration near the surface that is non-negligible in comparison to the magnitude of the distribution peak, a characteristic that is also observed in BFMC simulations for relatively low grafting densities.

By taking into account the total adsorbed amount $\Gamma = (100/16) \times \int \rho_{16\%}(z)\,dz$ we may calculate the reduced coverage $\sigma^* = \pi R_g^2/s^2$, where R_g is the radius of gyration of PS in toluene calculated using the relation $R_g = 0.0115 M_w^{0.595}$ [44] and s the interanchor distance calculated by $s = (N_A\Gamma/M_w)^{-1/2}$. The best fitted trial function in figure 7 gives $\Gamma = 2.4$ mg/m^2, $s = 80$ Å, and $\sigma^* = 6$ with a brush layer extension essentially six times larger than the radius of gyration of free PS chains in solution.

Previous studies[11,29,30] confirm that end-attached macromolecular layers characterized by reduced coverage values greater than 2 (where the onset of chain stretching occurs), tend to exhibit brush-like behavior and generally follow scaling laws and other predictions of SCF theory despite the fact that they are not strictly in the asymptotic limit of high surface coverage and strong stretching of the chains. The question of when tethered macromolecular chains can be regarded to have formed a "true" polymer brush has been recently discussed in detail by Brittain and Minko.[45] On the basis of a review of the literature, these authors suggest that the brush regime proper occurs for reduced coverage values, $\sigma^* > 5$. While the system we have investigated in the present study is obviously within the brush regime on the basis of this criterion, it is quite possible that the observed deviations of the free-end profile from eq 2 are due to the fact that the self-assembled brush under consideration lies in the intermediate region between the mushroom regime ($\sigma^* \leq 2$) and the asymptotic limit ($\sigma^* \geq 20$).[46] On the other hand, polydispersity effects, although small for our polymers ($M_w/M_n = 1.04$), may also play a contributory role in smearing the profile. It would be very interesting if one could in future perform a similar experiment with brushes that are prepared via "grafting-from" methods (i.e., polymerization techniques involving the *in situ* growth of chains on initiator-functionalized surfaces) such that much higher reduced coverage values (though with usually higher polydispersity) can be achieved.

Conclusions

In conclusion, we have performed the first direct measurement of the free-end distribution of polymer brushes in good solvent. The controlled labeling of the last 16% of the monomers of PS chains via selective deuterium enrichment permits the determination of the end-segment profile via neutron reflectivity. The determined profile apart from some deviations from the SCF theory shows that free ends are distributed throughout the brush layer and that the distribution peak is located within the brush and not at the height of the layer. Finally our results show that the labeling method employed together with the sensitivity provided by the neutron reflectivity technique could also be used in many other studies, as has been described recently,[47] where information for a specific part of a chain or a specific type of chain in a mixed system needs to be extracted.

References and Notes

(1) Napper, D. H. In *Polymeric Stabilization of Colloidal Dispersions*; Eds.; Academic Press: London, 1983.
(2) Fleer, G. J.; Cohen Stuart, M. A.; Scheutjens, J. M. H. M.; Cosgrove, T.; Vincent, B. *Polymers at interfaces*; Chapman & Hall: Bristol, U.K., 1993.
(3) Advincula, R. C.; Brittain, W. J.; Caster, K. C.; Rühe J. *Polymer Brushes: Synthesis, Characterization, Applications*; Wiley: New York, 2004.
(4) Zhao, B.; Brittain, W. J. *Prog. Polym. Sci.* **2000**, *25*, 677–710.
(5) Tirrel, M.; Levicky, R. *Curr. Opin. Solid State Mater. Sci.* **1997**, *2*, 668–672.
(6) Currie, E. P. K.; Norde, W.; Cohen Stuart, M. A. *Adv. Colloid Interface Sci.* **2003**, *100*, 205–265.
(7) Klein, J. *Annu. Rev. Mat. Sci.* **1996**, *26*, 581–612.
(8) Alexander, S. *J. Phys. (Paris)* **1977**, *38*, 983–986.
(9) De Gennes, P. G. *Adv. Colloid Interface Sci.* **1987**, *27*, 189–209.
(10) Hadziioannou, G.; Patel, S.; Granick, S.; Tirrell, M. *J. Am. Chem. Soc.* **1986**, *108*, 2869–2876.
(11) Field, J. B.; Toprakcioglu, C.; Ball, R. C.; Stanley, H. B.; Dai, L.; Barford, W.; Penfold, J.; Smith, G.; Hamilton, W. *Macromolecules* **1992**, *25*, 434–439.
(12) Taunton, H. J.; Toprakcioglu, C.; Fetters, L. J.; Klein, J. *Macromolecules* **1990**, *23*, 571–580.
(13) Alexander, S. *J. Phys. (Paris)* **1977**, *38*, 983–986.
(14) De Gennes, P. G. *Macromolecules* **1980**, *13*, 1069–1075.
(15) Zhulina, E. B.; Borisov, O. V.; Priamytsin, V. A. J. *Colloid Interafce Sci.* **1990**, *137*, 495.
(16) Milner, S. T.; Witten, T. A.; Cates, M. E. *Europhys. Lett.* **1988**, *5*, 413.
(17) Milner, S. T.; Witten, T. A.; Cates, M. E. *Macromolecules* **1988**, *21*, 2610. See also: Semenov, A. N. *Sov. Phys.—JETP (Engl. Transl.)* **1985**, *61*, 733. (*Zh. Eksp. Teor. Fiz.* **1985**, *88*, 1242).
(18) Wijmans, C. M.; Scheutjens, E. B.; Zhulina, E. B. *Macromolecules* **1992**, *25*, 2657–2665.
(19) Hirz, S. J. MS Thesis, University of Minnesota, **1986**.
(20) Carignano, M. A.; Szleifer, I. *J. Chem. Phys.* **1993**, *98*, 5006.
(21) Lai, P. Y.; Binder, K. *J. Chem. Phys.* **1991**, *95*, 9288–9299.
(22) Chakrabarti, A.; Toral, R. *Macromolecules* **1990**, *23*, 2016–2021.
(23) Laradji, M.; Guo, H.; Zuckermann, M. J. *Phys. Rev. E* **1994**, *49*, 3199–3206.
(24) Binder, K. *Monte Carlo and Molecular Dynamics Simulations in Polymer Science*; Oxford University Press: Oxford, U.K., 1995.
(25) Murat, M.; Grest, G. S. *Macromolecules* **1989**, *22*, 4054–4059.
(26) Murat, M.; Grest, G. S. *Macromolecules* **1993**, *26*, 3108.
(27) Auroy, P.; Mir, Y.; Auvray, L. *Phys. Rev. Lett.* **1992**, *69*, 93–95.
(28) Karim, A.; Satija, S. K.; Douglas, J. F.; Anker, J. F.; Fetters, L. J. *Phys. Rev. Lett.* **1994**, *73*, 3407–3410.
(29) Levicky, R.; Koneripalli, N.; Tirrell, M.; Satija, S. K. *Macromolecules* **1998**, *31*, 3731–3734.
(30) Kent, M. S.; Lee, L. T.; Factor, B. J.; Rondelez, F.; Smith, G. S. *J. Chem. Phys.* **1995**, *103*, 2320.
(31) Russell, T. P. *Mater. Sci. Rep.* **1990**, *5*, 171–271.
(32) Basu, J. K.; Boulliard, J. C.; Capelle, B.; Daillant, J.; Guenoun, P.; Mays, J. W.; Yang, J. *Macromolecules* **2007**, *40*, 6333–6339.
(33) Pispas, S; Hadjichristidis, N. *Macromolecules* **1994**, *27*, 1891.
(34) Battaglin, G.; Menelle, A.; Montecchi, M.; Nichelatti, E.; Polato, P. *Glass Technol.* **2002**, *43*, 203–208.
(35) Dorgan, J. R.; Stamm, M.; Toprakcioglu, C.; Jerome, R.; Fetters, L. J. *Macromolecules* **1993**, *26*, 5321–5330.
(36) Koutsioubas, A. G.; Spiliopoulos, N.; Anastassopoulos, D. L.; Vradis, A. A.; Toprakcioglu, C.; Priftis, G. D. *J. Polym. Sci., Part B: Polym. Phys.* **2006**, *44*, 1580–1591.
(37) Hiotelis, I.; Koutsioubas, A. G.; Spiliopoulos, N.; Anastassopoulos, D. L.; Vradis, A. A.; Toprakcioglu, C.; Menelle, A.; Sakellariou, G.; Hadjichristidis, N. *Macromolecules* **2008**, *41*, 7648–7655.
(38) Anastassopoulos, D. L.; Spiliopoulos, N.; Vradis, A. A.; Toprakcioglu, C.; Baker, S. M.; Menelle, A. *Macromolecules* **2006**, *39*, 8901–8904.

(39) Baker, S. M.; Smith, G. S.; Anastassopoulos, D. L.; Toprakcioglu, C.; Vradis, A. A.; Bucknall, D. G. *Macromolecules* **2000**, *33*, 1120–1122.
(40) Anastassopoulos, D. L.; Vradis, A. A.; Toprakcioglu, C.; Smith, G. S.; Dai, L. *Macromolecules* **1998**, *31*, 9369–9371.
(41) Carmesin, I.; Kremer, M. *Macromolecules* **1988**, *21*, 2819–2823.
(42) This is because each anchoring monomer occupies four lattice sites (i.e., a square) on the grafting plane and all adjacent squares are barred from being occupied by another anchoring monomer so that the maximum possible value of K/L^2 is 0.25.
(43) This is given by $\rho_{16\%}(z) = (\sum_{n=85}^{n=100} \rho_n(z))/16$.
(44) Roovers, J. E.; Toporowski, P. M. *J. Polym. Sci.* **1980**, *18*, 1907–1917.
(45) Brittain, W. J.; Minko, S. *J. Polym. Sci., Part A: Polym. Chem.* **2007**, *45*, 3505–3512.
(46) Baranowski, R.; Whitmore, M. P. *J. Chem. Phys.* **1995**, *103*, 2343–2353.
(47) Thomas, R. K. *Annu. Rev. Phys. Chem.* **2004**, *55*, 391–426.